metals

MDPI

Article

Towards Sustainable Battery Recycling: A Carbon Footprint Comparison between Pyrometallurgical and Hydrometallurgical Battery Recycling Flowsheets

Gert Van Hoof [1,*], Bénédicte Robertz [1] and Bart Verrecht [2]

[1] Umicore NV, Broekstraat 31, 1000 Brussel, Belgium; benedicte.robertz@eu.umicore.com
[2] Umicore NV, Watertorenstraat 33, 2250 Olen, Belgium; bart.verrecht@eu.umicore.com
* Correspondence: gert.vanhoof@eu.umicore.com

Abstract: The expected large growth in electric mobility presents challenges, such as requiring a very large amount of critical raw materials like nickel, cobalt, and lithium. Due to this expected growth significant amounts of production scrap from cell and battery manufacturing will be generated. Over the next decade, increasingly larger amounts of Li-ion batteries from electric vehicles will also reach their end-of-life. Hence, in order to close the loop, the development and industrialization of sustainable battery recycling flowsheets are key so that both production scrap and end-of-life batteries can be recycled back to their 'battery grade' building blocks. Battery recycling flowsheets are typically categorized into two categories: (1) 'Pyro-Hydro', a combination of battery smelting in a pyrometallurgical process, followed by the further refining of the alloy via hydrometallurgy; and (2) '(Thermo)mechanical-Hydro', a combination of (thermo)mechanical pretreatment and further hydrometallurgical refining of the resulting black mass. In this paper, a carbon footprint analysis is presented comparing these two battery recycling approaches: 'Pyro-Hydro' and 'Thermomechanical-Hydro', taking into account the impact of the latest evolutions in process technology and efficiency. To facilitate this comparison, a prospective LCA was carried out for the respective flowsheets. The quantitative analysis shows that 'Pyro-Hydro' leads to the lowest overall carbon footprint but also that both 'Pyro-Hydro' and 'Thermomechanical-Hydro' flowsheets have their challenges and opportunities for decarbonization. The inclusion of the fate of side streams such as graphite and electrolyte in the analysis is shown to be critically important in order to gain an objective and complete view.

Keywords: battery recycling; pyrometallurgy; hydrometallurgy; carbon footprint; lithium-ion batteries

Citation: Van Hoof, G.; Robertz, B.; Verrecht, B. Towards Sustainable Battery Recycling: A Carbon Footprint Comparison between Pyrometallurgical and Hydrometallurgical Battery Recycling Flowsheets. *Metals* **2023**, *13*, 1915. https://doi.org/10.3390/met13121915

Academic Editors: Denise Crocce Romano Espinosa, Daniel Assumpcao Bertuol and Amilton Botelho Junior

Received: 17 October 2023
Revised: 10 November 2023
Accepted: 17 November 2023
Published: 21 November 2023

1. Introduction

Due to the global mobility transformation, the electrification of the automotive sector will lead to a significant increase in the demand for battery raw materials, most notably Ni, Co, Li, and Cu [1]. This also necessitates planning for the end-of-life (EOL) stage of electric vehicle (EV) batteries. As the first generation of EVs is reaching their end-of-life, strong growth in EOL EV batteries is expected from the second half of this decade onwards [1]. In addition, the start-up of new facilities in the supply chain (cells/modules) for EV battery production will generate significant amounts of production scrap, from which the same valuable and critical raw materials metals will need to be recycled. This production scrap from battery production will form the bulk of the volumes for recycling in the coming years, but it is expected that by the end of the decade, the volume of EOL EV batteries will be the main contributor to volumes available for recycling.

Hence, in order to close the loop, the development and industrialization of sustainable battery recycling flowsheets are key so that both production scrap and EOL batteries can be recycled back to their 'battery grade' building blocks for new cathode materials and reduce the need for additional primary critical raw materials [2]. An additional driver for

recycling is the evolving regulatory framework, such as the EU Battery Regulation (BR) [3], which was published in July 2023. This will set the a.o. minimum criteria for the use of recycled content for key metals (Ni, Co, Li, and Cu) in batteries, minimum recovery yields for these metals in the recycling processes, a threshold for the carbon footprint of batteries, and responsible sourcing of battery materials.

Umicore is a materials technology company with a long history of recycling and refining, a.o. of precious metals in its Hoboken precious metals refining plant. Based on this recycling experience, in the mid-2000s, an early process for battery recycling (often referred to as Val'eas) [4] was developed and patented and shortly operated in Sweden. However, this process still required significant amounts of cokes and thus resulted in a relatively high carbon footprint. This early process also found its way into numerous Life Cycle Assessment (LCA) studies on battery recycling processes [5–7]. In 2011, an industrial pilot plant for battery recycling (7 kton/yr) was commissioned in Hoboken, Belgium, using Umicore's proprietary Ultra High Temperature (UHT) technology instead of a shaft furnace technology. Initially, the plant recycled portable and first-generation EV batteries (NiMH, . . .), but since future market volumes are dominated by the newer generations of EV batteries and production scrap, which are vastly different, both in form factor and chemistry, the process was adapted and optimized to be ready for these upcoming volumes. Due to these optimizations, the process has now become autogenous via embedded chemical energy in the batteries, significantly reducing the carbon footprint. A novel lithium recovery method was also patented and incorporated [8]. This updated industrial pilot will support upscaling towards a larger industrial facility [9], which will use a combination of proprietary pyro- and hydrometallurgical processes to recycle both production scrap and end-of-life batteries. We will refer to this new process in this paper as the 'Pyro-Hydro' process.

The sustainability and circularity of battery recycling have been extensively investigated in the recent scientific literature. Velázquez-Martinez et al. [5], Brückner et al. [6], and Doose et al. [7] describe several metallurgical routes and associated advantages and challenges for recycling lithium-ion batteries (LIB), a major technology in EV batteries. Rajaeifar et al. [10] use LCA to compare various pyrometallurgical recycling processes. In all of these papers, reference is made to the outdated Umicore patented Val'éas process [4], which is no longer used. As this patent serves as the basis for energy and carbon footprint calculations in comparison to alternative recycling process routes, the carbon footprint results of pyro (or smelting) processes are often overstated and do not reflect the latest process evolutions.

Hence, the key objective of this paper is to present an updated carbon footprint comparison (from a prospective LCA study) for battery recycling processes on an industrial scale and reflect the current state of the art, both for the 'Pyro-Hydro' process and for a 'Thermomechanical pretreatment-Hydro' process (i.e., a recycling process combining mechanical treatment, pyrolysis, and hydrometallurgy). A second objective is to illustrate the importance of accurately assessing the fate of the different side streams, such as graphite and electrolyte, in order to gain a complete and objective view.

2. Materials and Methods

We start this chapter with a description of the process technology applied in both flowsheets (Section 2.1). This information is needed to understand the choices on system boundaries and data selection of valuable outputs, described in the methodological approach of the LCA study (Section 2.2).

2.1. Battery Recycling Flowsheets

2.1.1. Casing Removal (Dismantling/Case Removal/Mechanical Shredding)

Before entering a battery recycling flowsheet, EOL battery packs are typically manually or (semi-) automatically dismantled to the module level [11]. Given that this step is not discriminative for the flowsheets under study, it is excluded from the system boundary, and

the LCA model starts from modules. Additionally, in order to facilitate recovery of module casing materials (e.g., Al, steel, plastics, etc.), an optional casing removal step to dismantle modules to cell level can be added. This is the base scenario in this LCA study and results in the following side fractions for both flowsheets: copper wires, steel casing, aluminum casing, and a plastic fraction. While case removal is also not discriminative between the 2 flowsheets and technically not needed for the 'Pyro-Hydro' flowsheet, it was added to evaluate both flowsheets on a similar basis and to align with most other LCA studies as these side fractions are important for credits to the system.

2.1.2. Pyro-Hydrometallurgical Flowsheet ('Pyro-Hydro')

Figure 1 visualizes the 'Pyro-Hydro flowsheet'. After the casing removal step, the cells are fed into the pyrometallurgical process. This process ensures a robust separation between Ni, Co, Cu (which end up in a pure alloy for further hydrometallurgical refining), Al, Fe, and a fraction of the Mn and impurities (which go to the slag phase). In the smelting process, the remaining Al (~5 wt% of the feed, from the cathode foil) and carbon (mainly graphite from the anode and electrolyte) in the feed serve two purposes: (1) they act as a reducing agent, hence ensuring the separation between Ni, Cu and Co, and Al, Fe, and other impurities (which go to the slag), and (2) they deliver the energy for the pyro process as this reaction is exothermic, hence obviating the need for an external energy source. The gases from the pyrometallurgical step are rich in CO_2 (from the graphite and electrolyte). Heat exchangers recover the heat from the flue gas, producing steam sufficient to supply steam to all subsequent steps. Therefore, the entire flowsheet is 'steam neutral'.

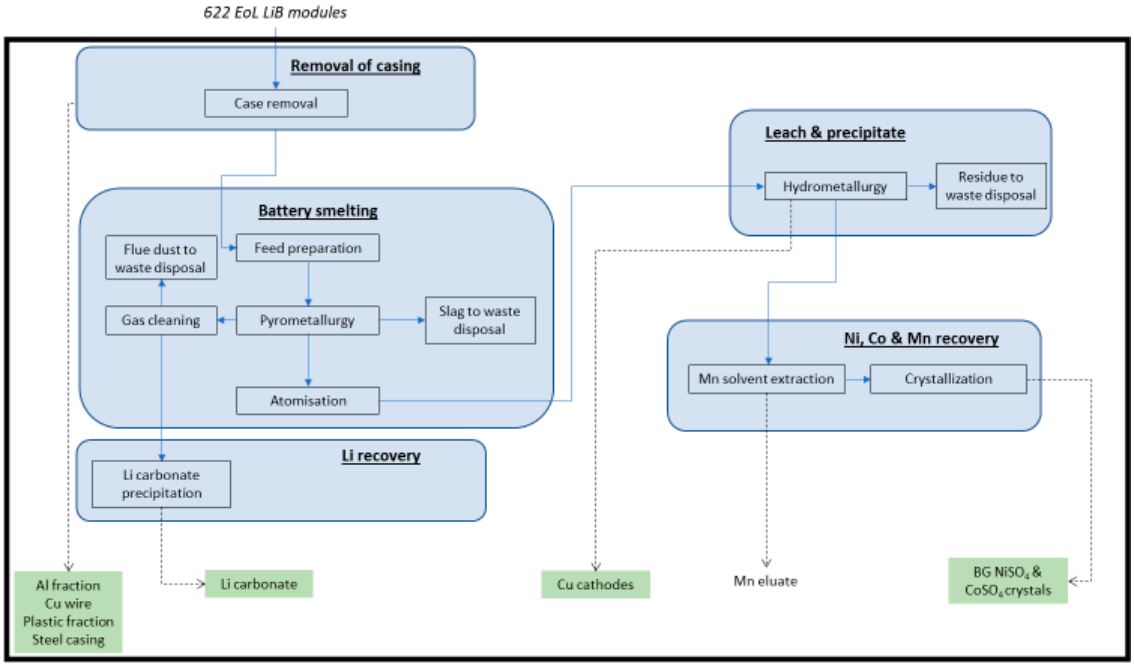

Figure 1. Pyro-hydrometallurgical recycling flowsheet ('Pyro-Hydro'). Legend: black thick line = system boundaries, blue arrows internal flows, green squares = credits connected with dotted lines.

In the pyro process, Li reports to the flue dust using a patented fuming process [8]. Afterward, Li is recovered from the flue dust via reaction with Na_2CO_3 in order to form technical grade (TG) Li_2CO_3, which can be refined further to battery grade LiOH. After Li recovery, the remaining flue dust is disposed of as inert waste. For the purpose of the LCA and taking a worst-case approach by assigning a burden to the waste treatment, the slag is modeled as an inert waste. However, higher value-added applications for this clean slag are possible.

The alloy, rich in Ni, Co, and Cu, is atomized and fed to a hydrometallurgical process using sulfuric acid to dissolve all metals. The leaching residue (a.o. containing Fe) is dis-

posed of as hazardous waste. Copper in solution is removed via electrowinning, resulting in high-purity copper cathodes. The remaining solution is sent to a solvent extraction process to remove manganese (as $MnCl_2$). It is possible to convert the $MnCl_2$ to $MnCO_3$, which can then be further purified to a quality suitable for use in batteries. However, currently, this Mn solution is not valorized (reflecting current industry practice), and conversion of this stream to $MnCO_3$ has not been considered in this paper. We have therefore chosen to allow $MnCl_2$ to leave the system without burden or credits. The same reasoning applies to the thermomechanical pretreatment–hydrometallurgical flowsheet presented below. The concentrated solution of nickel and cobalt sulfate is crystallized to form Ni and Co sulfate (hexahydrate for Ni, heptahydrate for Co).

2.1.3. Thermomechanical Pretreatment–Hydrometallurgical Flowsheet

The representative 'Thermomechanical-Hydro' flowsheet used in this study is based on Umicore's market understanding and is largely in line with the findings of Neuman et al. [12].

NMC modules are fed through a mechanical shredding step and coarse fractions are manually removed (Figure 2). Fractions obtained after this step are:

- Copper wires interconnecting the cells (removal of casing);
- Steel casing (removal of casing);
- Plastics (removal of casing);
- Aluminum casing (removal of casing);
- The current collectors from the cells result in a Cu-Al fraction (pretreatment);
- Black mass (pretreatment) comprising most of the anode and cathode materials, which is fed into a hydrometallurgical process.

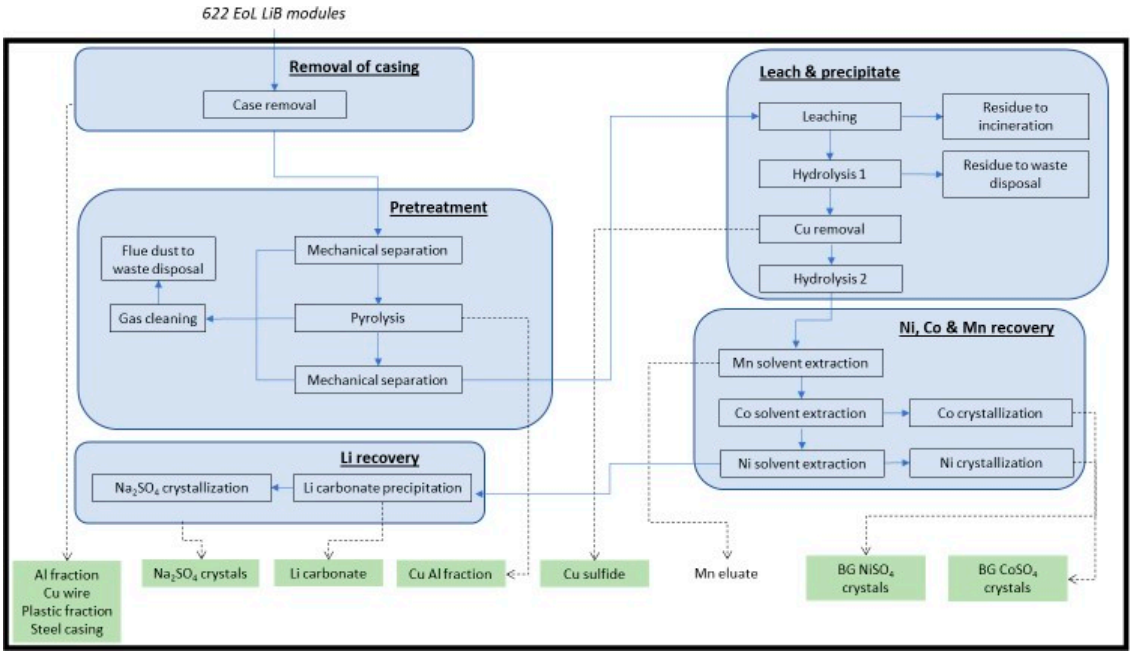

Figure 2. Thermomechanical-Hydrometallurgical recycling flowsheet. Legend: black thick line = system boundaries, blue arrows internal flows, green squares = credits connected with dotted lines.

In order to deal with the complex feed mix—predominantly electrolyte-containing EOL batteries—that is expected in the future, thermal treatment step (pyrolysis) is required. It is important to clearly distinguish between pyrolysis and pyrometallurgical processes: pyrolysis refers to thermal processes, typically run at temperatures between 200 and 800 °C, and mainly result in removal (via oxidation) of electrolyte/organics as a gas phase. This contrasts with pyrometallurgy (as part of the pyro-hydro flowsheet as described in Section 2.1.2), which refers to ultra-high temperature smelting processes (well above

1000 °C), meaning all elements enter a liquid state which enables a separation between the noble and less noble elements, which report, respectively to the alloy and slag.

The pyrolysis step also enables improved separation between the cathode materials (Ni, Co, Mn, and Li) and cathode and anode foils (Cu and Al) as it degrades the PVDF binder. Therefore, it is essential to facilitate further hydroprocessing of the produced black mass [6]. Gases and dust from the mechanical separation steps and the pyrolysis are sent to gas cleaning units. They are rich in CO_2 from the oxidation of various carbon-containing elements in the cells. Flue dust is collected and disposed of as an inert waste.

The 'leach & precipitate' block of the flowsheet consists of 4 steps: leaching, a first hydrolysis step, removal of copper, and final hydrolysis. The black mass coming out of the pretreatment is leached with sulfuric acid and reduced with hydrogen peroxide. The residue from the leaching process is rich in carbon (from the graphite in the cells). This residue, with a high calorific value due to its high carbon level, is modeled to be incinerated following the waste hierarchy in the EU Waste Framework Directive [13]. An alternative route could also be its use as a reducing agent in the steel industry. At present, no other industrially viable recovery method for carbon has been published.

The residue from the first hydrolysis, containing Fe and Al, is landfilled. Copper is removed to increase the efficacy of the subsequent solvent extraction. Copper leaves the system as copper sulfide, which may be used as input into Cu smelting. The quantity of copper sulfide is stoichiometrically calculated based on the total quantity of copper. A second hydrolysis is the last step in the 'leach & precipitate' block. Its residue is internally recycled into the leaching step. After the second hydrolysis, the solution is concentrated on Ni, Mn, and Co ions.

In order to produce battery-grade end products, the concentrated Ni, Co, and Mn solution is fed to 3 solvent extraction processes in which first manganese is removed, followed by cobalt and nickel. Manganese is concentrated in the extraction process as $MnCl_2$. Similar to the pyro-hydrometallurgical flowsheet and reflecting the current industry practices, this flow leaves the system without burden or credit.

The nickel and cobalt sulfate concentrated solutions from the respective solvent extractions are crystallized (hexahydrate for $NiSO_4$, heptahydrate for $CoSO_4$).

The eluate from the nickel solvent extraction is rich in lithium. It is reacted with soda, precipitated, and dried, leaving the system as technical-grade lithium carbonate. The remaining sodium sulfate-rich solution is also crystallized.

2.2. LCA Study Approach

An attributional prospective LCA study is performed with the goal of comparing two specific process routes for recycling EOL LIB batteries. This study is a prospective study since the primary data on both flowsheets are from an engineering model based on long-term operational and industrial experience on the individual unit processes (both pyrometallurgical and hydrometallurgical), and its results were used for the investment decision. For confidentiality reasons, the full inventory table cannot be disclosed. The functional unit is the recycling of 100 kton of EOL LIB modules in Europe, and the LCA model follows the cut-off approach, meaning the EOL LIB modules enter the recycling plant free of burden. An average EU electricity grid composition was taken, and transport distances in the supply chain were generically modeled. The LCA model was built in GaBi LCA software (v 10.7, Sphera, Leinfelden-Echterdingen, Germany), using primarily GaBi background datasets for energy and chemicals. Data on Co (production year 2012) and Ni (production year 2017) originated from Cobalt Institute [14] and Nickel Institute [15] and represent industry averages. Ecoinvent 3.4 [16] data were used to close data gaps.

The Environmental Footprint impact assessment methodology [17] was applied, as developed by the EU Joint Research Center (JRC) in the context of the Product Environmental Footprint (PEF) and Organizational Environmental Footprint (OEF) [18]. Only impact categories (9 in total) with robustness levels I and II were taken. In this paper, we only show results on climate change (carbon footprint) to allow for sufficient discussion space. Carbon

footprint results are often broken down into scope 1, 2, and 3 contributions, following the greenhouse gas (GHG) protocol [19]. Scope 1 represents a reporting organization's direct GHG emissions; scope 2 is associated with a reporting organization's emissions from generation of electricity, heating/cooling, or steam purchased for own consumption; scope 3 covers a reporting organization's indirect emissions other than those under scope 2.

This study follows the ISO standard for LCA [20] and was critically reviewed by the Öko-Institut (M. Buchert & J. Sutter).

2.2.1. Feed Characterization

The LCA study was performed on a single feed composition (NMC622). This is a simplification of reality since the plant is designed to deal with different LIB compositions. However, this simplification allows us to perform mass balance checks and yield calculations on the key metals (Ni, Co, Li, and Mn). Table 1 provides an overview of the composition of the feed material in the recycling process. The data in Table 1 are from a Umicore study analyzing various representative modules with NMC622 cells and hence represent a hypothetical average feed into a recycling process. Compared to data via the GREET model from Argonne National Laboratory [21], this hypothetical average feed is different on module casing (steel and aluminum), while differences in cell composition are minimal.

Table 1. Composition of the NMC models entering the recycling process.

NMC Modules	**NMC Cells**		**Quantity for 100 kton NMC Modules**
Composition (wt%)	**Composition (wt%)**	**Carbon (wt%)**	**ton**
Cells (75%)			
	Copper foil (7.1%)	-	5310
	Aluminum foil (5.0%)	-	3150
	Active cathode material (43.0%)	-	32,273
	Graphite (19.1%)	100%	14,347
	Carbon black (2.3%)	100%	1723
	Binder: PVDF (2.7%)	37.52%	2037
	LiPF6 (2.1%)	-	1546
	Electrolyte (14.3%)	45.66%	10,763
	Separator (2.2%)	92.26%	1641
	Pouch casing (1.4%)	-	1040
Cu wires (0.1%)		-	62
Stainless steel (7.2%)		-	7191
Aluminum casing (10.8%)		-	10,804
Plastics (6.9%)		65.48%	6882

2.2.2. System Boundaries: Definition of Burdens and Credits

The selection of the system boundaries in LCA recycling models is of critical importance. On the one hand, there is a burden of the recycling activity, and on the other hand, recycling generates valuable outputs that displace the use of primary materials, here defined as credits. In this study, we report burdens and credits transparently since overall results may strongly depend on the choices made in the system boundaries.

In both recycling flowsheets, EoL LIB modules enter the system boundaries free of burden. Both flowsheets consist of 5 main modules (Figures 3 and 4 show this for the 'Pyro-Hydro' and the 'Thermomechanical—Hydro' flowsheet, respectively). Each of the main modules generates specific output flows which generate credits to the system (in blue in Figures 3 and 4). Treatment of waste streams (hazardous waste incineration or landfill) is also included in the system boundaries. In the 'Thermomechanical-Hydro' flowsheet, the leaching step results in a residue that is high in carbon content (from the graphite in the LIB modules). Due to this high carbon content and associated calorific value, the EU

waste hierarchy requires disposing of this waste with energy recovery. Other waste flows are inert in nature and can be landfilled.

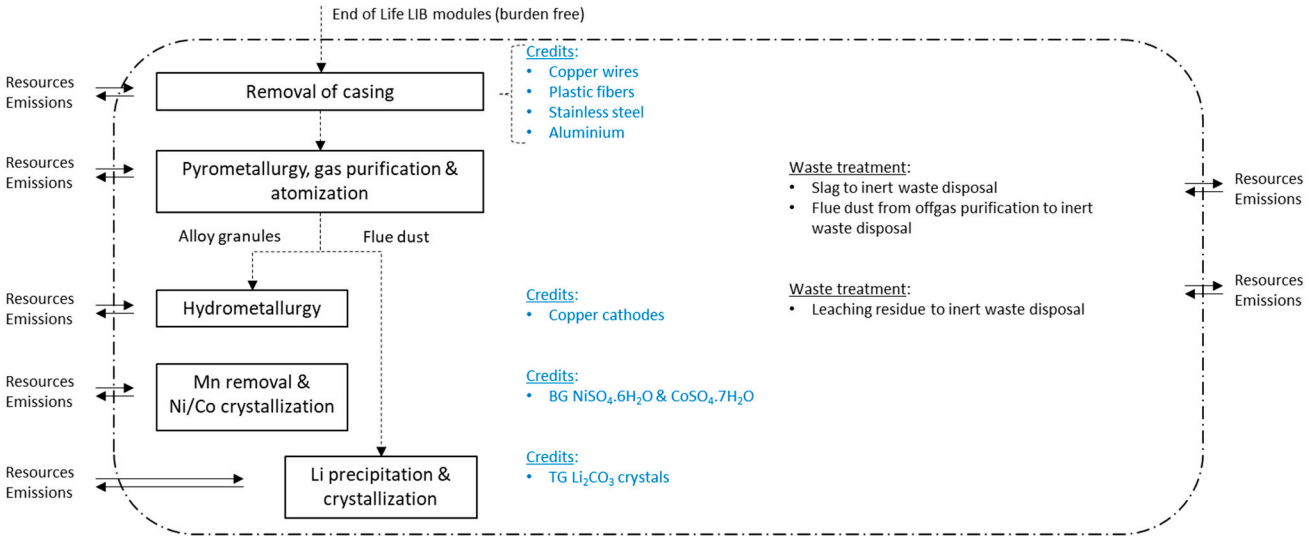

Figure 3. System boundaries Pyro-Hydro flowsheet. Credits from avoided products in blue.

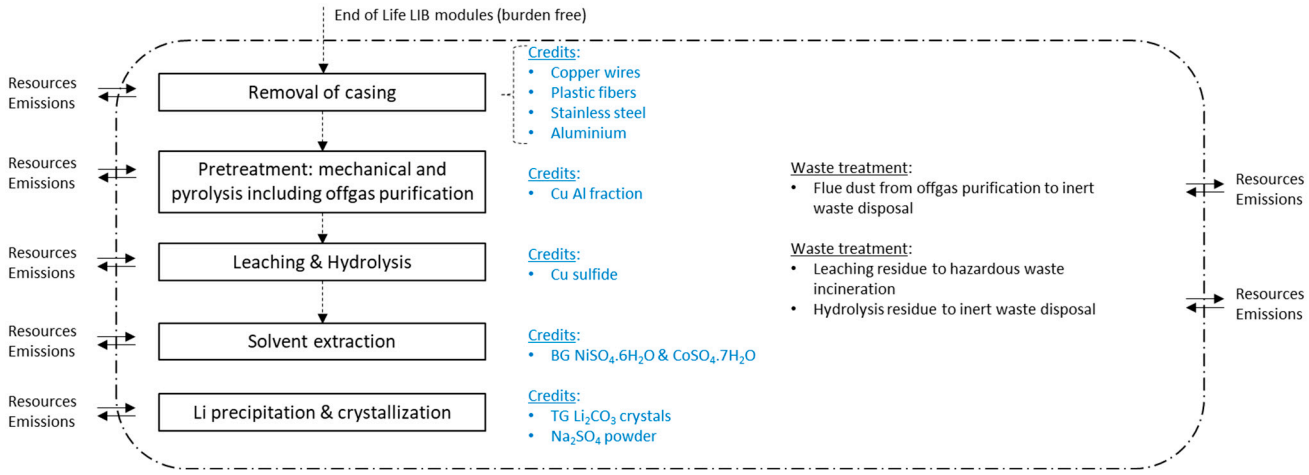

Figure 4. System boundaries Thermomechanical-Hydro flowsheet. Credits from avoided products in blue.

Transport of materials and waste is included. Packaging and the end-of-life treatment of used packaging are excluded. This is in line with guidance on cut-off criteria provided in the Global Battery Alliance rulebook [22].

3. Results and Discussion

As explained in the section on system boundaries, battery recycling generates an environmental burden from the use of resources and emissions in the various process steps. However, it also results in valuable products that replace materials produced from primary sources, thereby creating credit. When the balance between the burden and the credits is negative, recycling constitutes an improvement. The results of the burden and credits are discussed separately.

3.1. Climate Change Burden of Recycling

The results are analyzed by breaking down the carbon footprint into their contributions following the greenhouse gas protocol (i.e., scope 1, 2, and 3), as well as into their contributions related to the process steps for both flowsheets (Figures 5 and 6, respectively).

The former allows us to understand where in the value chain emissions originate (indicating potential for decarbonization), while the latter helps to clarify how technology differences between both flowsheets result in a different carbon footprint profile. Figure 5 shows that a combination of pyro- and hydrometallurgy results in the lowest overall footprint, at 2.07 kg CO_2e/kg module input, vs. 2.64 kg CO_2e/kg module input for the combination of thermomechanical pretreatment and further hydrometallurgical refining of the black mass.

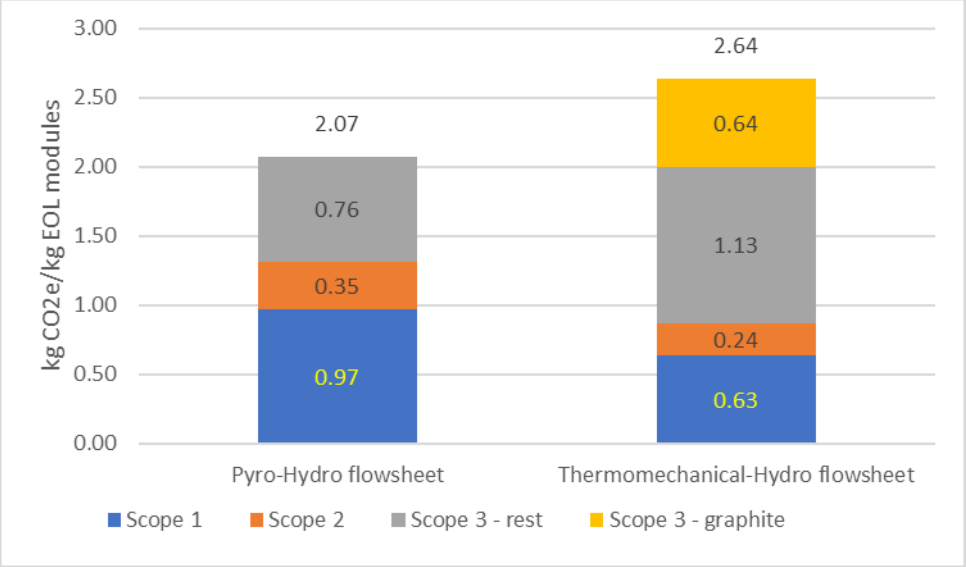

Figure 5. Carbon footprint from the recycling operation (excluding credits) for the 'Pyro-Hydro' and 'Thermomechanical-Hydro' battery recycling broken down by their contribution to the GHG Protocol scopes.

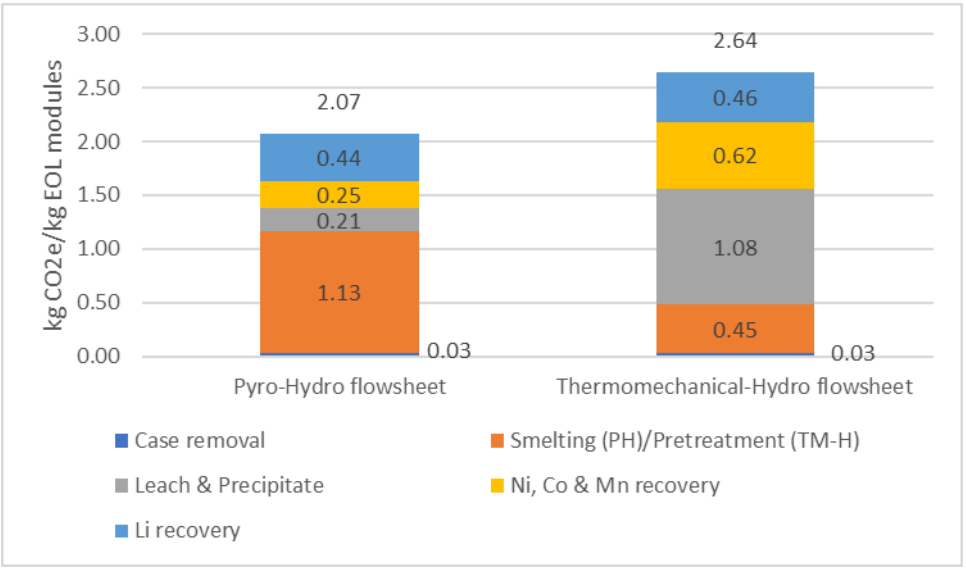

Figure 6. Carbon footprint from the recycling operation (excluding credits) for the 'Pyro-Hydro' and 'Thermomechanical-Hydro' battery recycling: breakout by process step for both flowsheets.

The carbon footprint profiles of the different flowsheets are vastly different: 'Pyro-Hydro' has larger scope 1 emissions (0.97 kg CO_2/kg module input), the carbon (electrolyte, graphite) contained in the battery generates the energy for the process and acts as a reducing agent, and is converted into CO_2 scope 1 emissions. The 'Thermomechanical-Hydro' flowsheet scope 1 emissions are lower (0.63 kg CO_2/kg module input) and are mainly linked to the combustion of natural gas and electrolyte in the pyrolysis pretreatment.

Scope 2 emissions—linked to the carbon footprint of purchased energy—are 0.35 and 0.24 kg CO_2e/kg module input for the 'Pyro-Hydro' flowsheet and 'Thermomechanical-Hydro' flowsheet, respectively. This difference is mainly linked to the electrowinning of Cu in the 'Pyro-Hydro' flowsheet to valorize the Cu as copper cathodes. In the 'Thermomechanical-Hydro' flowsheet, the copper is valorized as copper sulfide.

The scope 3 emission profile also shows a different picture for the two flowsheet approaches, with 0.76 kg CO_2e/kg module input for the 'Pyro-Hydro' flowsheet vs. 1.77 kg CO_2e/kg module input for the 'Thermomechanical-Hydro' flowsheet. This difference can be explained by the different flowsheet designs. First, a high amount of impurities is removed via the slag in the 'Pyro-Hydro' flowsheet, leading to a pure alloy and making the subsequent hydro flowsheet less complex. This results in a lower consumption of reagent compared to the 'Thermomechanical-Hydro' combination. The latter relies more on reagent-intensive solvent extraction processes. Taking into account the full scope of leaching and neutralizing agents, the net impact on scope 3 emissions is lower for the 'Pyro-Hydro' flowsheet (0.76 kg CO_2e/kg EOL module) than for the 'Thermomechanical-Hydro' flowsheet (1.13 kg CO_2e/kg EOL module). Second, graphite ends up in the leach residue in the 'Thermomechanical-Hydro' flowsheet. Due to the waste hierarchy in Europe, this residue cannot be landfilled and is burned at an external waste incinerator, resulting in CO_2 emissions. Hence, the fate of carbon (graphite/electrolyte) embedded in the batteries is similar in both flowsheets: in the 'Pyro-Hydro' flowsheet, carbon delivers the energy for the recycling process and acts as a reducing agent, contributing to scope 1 GHG emissions, while in the 'Thermomechanical-Hydro' flowsheet, the contribution of this embedded carbon is split between scope 1 GHG emissions (electrolyte oxidation in the pyrolysis process) and scope 3 (graphite in the leach residue is incinerated). This also clearly highlights the importance of graphite recycling in order to make battery recycling more sustainable. However, challenges remain: the technology readiness level of graphite recycling is currently very low, and both the economics and environmental impact of graphite recycling require further analysis [11,23,24], which is outside the scope of this paper. However, our analysis also confirms the importance of looking at the different side streams generated in the recycling processes to understand the fate of the carbon flows beyond the actual recycling processes.

A break-out of the carbon footprint by process step is given in Figure 6. The largest differences are observed with the smelting and pretreatment step (1.13 vs. 0.45 kg CO_2e/kg EOL modules). This is largely attributed to the carbon footprint from the oxidation of graphite and electrolyte taking place in different process stages in both flowsheets (smelting for the 'Pyro-Hydro' flowsheet, leach & precipitate for the 'Thermomechanical-Hydro' flowsheet). The figure also shows that the combined steps in both flowsheets (smelting and leach and precipitate or pretreatment and leach and precipitate) are not very different in terms of absolute carbon footprint (1.34 vs. 1.53 kg CO_2e/kg EOL modules for the 'Pyro-Hydro' and 'Thermomechanical-Hydro' flowsheet, respectively). Due to a simplified hydrometallurgy in the 'Pyro-Hydro' flowsheet, the metal recovery contribution is lower as compared to the 'Thermomechanical-Hydro' flowsheet (0.25 vs. 0.62 kg CO_2e/kg EOL modules for the 'Pyro-Hydro' and 'Thermomechanical-Hydro' flowsheet, respectively). Contributions from the Li recovery are comparable for both flowsheets.

3.2. Material and Energy Recovery

When looking at recovered materials from the recycling process, it is important to understand their nature and grade to correctly assign displaced materials, resulting in credits. Hence, this section lists some considerations on the Co, Ni, Mn, Li, and Cu flows in both flowsheets.

Generally, yields for the 'Thermomechanical-Hydro' flowsheet are 10% lower for Ni and 9% lower for Co due to losses in the mechanical pretreatment [6].

Li recovery is slightly more efficient (2%) in the 'Pyro-Hydro' flowsheet compared to the 'Thermomechanical-Hydro' flowsheet. For both flowsheets, a technical grade Li

carbonate has been considered the endpoint in this LCA, which needs further refining to battery grade Li carbonate or LiOH.

Mn losses in the 'Pyro-Hydro' flowsheet are higher since a significant fraction is lost in the slags. Overall Mn recovery is 74% lower for the 'Pyro-Hydro' flowsheet compared to the 'Thermomechanical-Hydro' flowsheet. Should credits be assigned to Mn, this may create a benefit for the 'Thermomechanical-Hydro' flowsheet (see next section). Since Mn now leaves the system without any credit or burden, this difference is not accounted for.

For the 'Thermomechanical-Hydro' flowsheet, most (64%) of the Cu is separated in the pretreatment and valorized as a low-quality Cu-Al fraction, which will often be processed further in a Cu smelter. The remaining Cu flows through the 'Thermomechanical-Hydro' flowsheet and is separated as CuS during leaching and precipitation. For the 'Pyro-Hydro' flowsheet, all Cu is collected in the alloy and valorized as high-quality Cu cathodes. Overall, Cu recovery is 19% more efficient in the 'Pyro-Hydro' flowsheet.

Graphite is not recycled in either flowsheet. However, as explained in Section 2.1.2, the energy from the reduction in the 'Pyro-Hydro' flowsheet is recovered and makes the overall process steam neutral (i.e., no additional fuels are needed for the production of steam). Graphite in the leaching residue from the 'Thermomechanical-Hydro' flowsheet is treated in a waste incinerator. While the waste incinerator may also recover the energy, this is not accounted for in the model.

3.3. Credits from Recycling in Climate Change Terms

We can group the valorized materials from the recycling into two categories. The first category includes materials that displace primary materials in new cathode materials, thereby closing the loop for use in the same application (closed-loop credits). Ni sulfate, Co sulfate, and Li carbonate (as a precursor for battery grade Li carbonate or LiOH) fit into this category. The second category includes materials not recycled back into cathode materials but in other applications (open-loop credits). To this category, the following metals and materials belong Al (from case removal), Cu (wires from case removal, cathodes from the 'Pyro-Hydro' flowsheet, Cu-Al fraction and CuS from the 'Thermomechanical-Hydro' flowsheet), sodium sulfate (from 'Thermomechanical-Hydro' flowsheet), stainless steel (from case removal) and plastics (from case removal). We also discuss two specific cases: Mn and graphite. These two materials have a different fate in both flowsheets (Sections 2.1.2 and 2.1.3) and are further discussed from a credit accounting point of view.

The baseline scenario assumes the recycling facility will be based in Europe. Therefore, datasets selected for the credit calculation should also follow an EU scenario when it is well known that there are regional differences. This is the case for stainless steel scrap and aluminum (leading to lower credits in Europe as compared to their production in China).

In absolute terms, total credits are largest with the 'Pyro-Hydro' flowsheet (Figure 7). Closed-loop credits are larger for the 'Pyro-Hydro' flowsheet due to the more efficient recovery of Ni, Co, and Li.

It should be noted that the model did not assign credits to the recovery of Mn, which is significantly higher in the 'Thermomechanical-Hydro' flowsheet. As explained in Section 2.1.2, Mn leaves the system as $MnCl_2$, which could be reacted to $MnCO_3$, which may be a precursor for the production of battery-grade $MnSO_4$. The sensitivity of this assumption has been tested. It is assumed that $MnCO_3$ would displace a manganese concentrate (42.4% Mn) produced from mining and beneficiation [16], which has a carbon footprint of 0.019 kg CO_2e/kg Mn concentrate. This leads to a total credit of 124-ton CO_2e. However, the carbon footprint of the soda to react $MnCl_2$ in solution to $MnCO_3$ (burden of the process) is 7765-ton CO_2e. Therefore, the recovery of the Mn does not lead to a net benefit in carbon terms. Current industry practice is that Mn is not recovered.

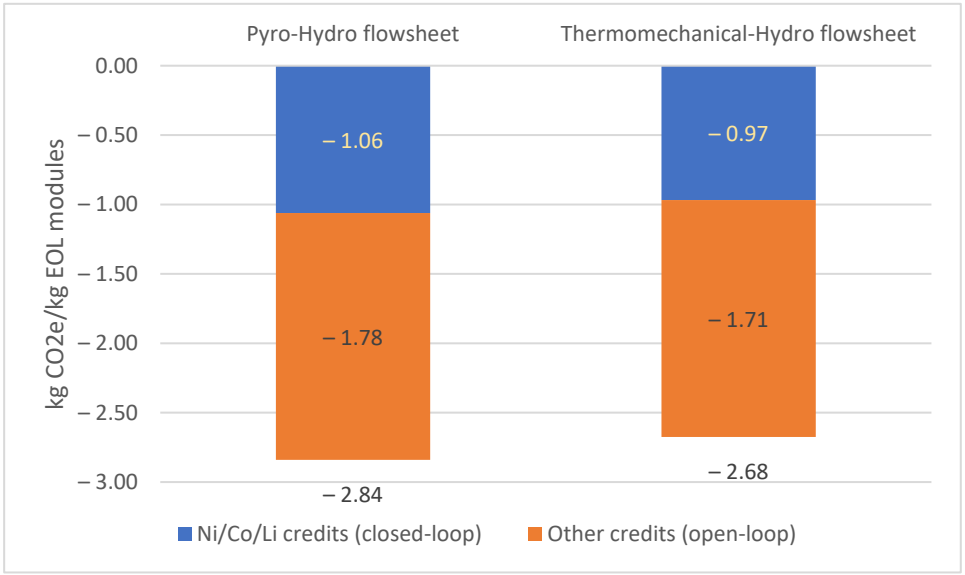

Figure 7. Carbon footprint credits for the various types of materials valorized in both flowsheets.

The energy recovery from graphite incineration in the residue from the 'Thermomechanical-Hydro' flowsheet may be another point of discussion. As stated before, due to the European waste hierarchy, the modeling of this waste flow with high calorific value assumes hazardous waste incineration. Energy may be recovered as heat or electricity in those installations. However, since fees need to be paid for its safe waste disposal (no economic value), it is commonly accepted to not account for credits to this energy recovery. In the 'Pyro-Hydro' flowsheet, the energy is recovered in the battery recycling process, which is further used in hydrometallurgy and, therefore, an inherent part of the operational design. Additionally, energy balances indicate that there is excess energy that needs to be effectively managed in the smelting operation. We did not assign any credit from displaced fuels for the energy recovery in the smelting operation. For consistency reasons, credits for the displacement of fuels should, therefore, not be assigned when the graphite residue would be used in, e.g., steel making.

3.4. Net Climate Change Results

Table 2 summarizes the net climate change results for both flowsheets when considering the burden and credit impacts.

Table 2. Summary of the carbon footprint results for both flowsheets.

kg CO_2e/kg EOL Modules	'Pyro-Hydro'	'Thermomechanical-Hydro'
Burdens	2.07	2.64
Credits	−2.84.	−2.68
Net result	−0.77	−0.03

The net balance between recycling burdens and credits is negative for both flowsheets (Table 2). This indicates that recycling EOL LIB modules is overall a better option in terms of carbon footprint.

Looking into the details of both flowsheets, the net climate change results are significantly lower for the pyro-hydro flowsheet (−0.77 vs. −0.03 kg CO_2e/kg EOL modules for 'Pyro-Hydro' vs. 'Thermomechanical-Hydro'). This is due to larger credits and lower burdens for the Pyro-Hydro flowsheet. As discussed in Section 3.3, the higher recovery from Mn in the 'Thermomechanical-Hydro' flowsheet compared to the 'Pyro-Hydro' flowsheet does not change this conclusion.

3.5. Comparison of Results with Literature Data

As stated in the introduction, the objective of this paper is to compare two state-of-the-art battery recycling processes in industrial practice today: the 'Pyro-Hydro' process and the 'Thermomechanical-Hydro' process combining mechanical treatment, pyrolysis, and hydrometallurgy. The results are compared with data in the literature. While a detailed comparison would require going into depth into applied study methodologies and data sources, going beyond the scope of this paper, this section aims to shed light on key differences and similarities.

Rajaeifar et al. [10] describe battery recycling processes using pyrometallurgy. The processes are based on direct current plasma technology. However, the benchmark scenario is using the outdated Val'eas process [4]. The cell chemistry in the work by Rajaeifar is NMC111, and the starting material is also EOL LIB modules. On the burden site, the carbon footprint is higher than in our study (Table 3). This is not a surprise since the Val'eas process relies on cokes. The total scope 1 carbon footprint (combustion of graphite, electrolyte, and cokes) is, hence, 2.17 kg CO_2e/kg. The pyrometallurgical process in our study is autogenous in energy terms, and the combustion of graphite and electrolyte leads to 0.64 kg CO_2e/kg. On the credit side, higher credits are observed with Rafaeijar. This can be explained by the choices of avoided products where, in the closed-loop model, data for $Ni(OH)_2$ and LiCoO2 from GREET [21] are used. In addition, metal recovery yields are different, and credits for Fe and slag as aggregate are used. While Mohr et al. [25] also refer to the Val'eas data [4] for pyrometallurgical processes, the actual LCI data are from 2007, which is why we conducted no further comparison.

Table 3. Carbon footprint results for the 2 recycling flowsheets compared with data in the literature.

		Burden kg CO_2e/kg	**Credit** kg CO_2e/kg
Pyro-Hydro flowsheet	Rafaeijar et al. [10]	2.84	−3.61
	This study	2.07	−2.84
Thermomechanical-Hydro flowsheet	Buchert and Sutter [26]	1.93 [a]	−2.33 [a]
	This study	2.64	−2.68

[a] Excluding the values of inbound transport and dismantling for consistency reasons in system boundaries.

For the 'Thermomechanical-Hydro' flowsheet, we compare the results from this study with those from Buchert and Sutter [26]. This study includes the burdens of inbound transport of materials and the dismantling step. With the exception of these two steps, there is a good consistency between both studies in terms of system boundary choices. The Buchert and Sutter results in Table 3, therefore, do not include the inbound transport and dismantling. On the burden side, results in the present study are higher (2.64 vs. 1.93 kg CO_2e/kg). The geographical boundary differences (Germany vs. average EU) may have some impact on electricity grids, even though electricity is not the main driver. Scope 3 carbon footprint contributions (including emissions from reagents and chemicals) in the 'Thermomechanical-Hydro' flowsheet are significant, which is why we hypothesize that the use of a different background database [27] in the Buchert & Sutter study [26]) is the main reason for the observed difference. Credits are also lower in the study by Buchert and Sutter despite strong comparability in terms of valorized fractions. The choice of the Co dataset may partly explain the lower value: the Co data source in the study from Buchert and Sutter is from ecoinvent 3.1, which is a factor 3 lower than the value reported by Cobalt Institute. The importance of recycled fractions of aluminum and plastic in the open-loop credits for climate change is consistent with observations in the study by Buchert and Sutter.

4. Conclusions/Summary

In this paper, carbon footprint results from a life cycle assessment study are compared for a Pyro-Hydrometallurgical and a Thermomechanical-Hydrometallurgical flowsheet to

recycle end-of-life modules from lithium-ion batteries in a European geographical context. These processes have been chosen as they represent the industrial practice today. In both cases, the impact of the latest evolutions in process technology and efficiency has been taken into account.

The quantitative analysis highlights that 'Pyro-Hydro', a combination of pyro and hydrometallurgical battery recycling, leads to the lowest overall carbon footprint. Both flowsheets enable the valorization of different materials. When taking the associated credits from this valorization into account, both flowsheets have a net negative carbon footprint result, though significantly more negative for the 'Pyro-Hydro' flowsheet. This net negative impact indicates the environmental benefit from battery recycling. Both flowsheets differ significantly in the source of GHG emissions associated with the recycling operation. The 'Pyro-Hydro' flowsheet has a higher scope 1 (direct) carbon footprint, linked to the combustion of carbon (graphite/electrolyte) embedded in the batteries, which provides the energy for the autogenous smelting process and acts as a reducing agent. The scope 3 (indirect up-stream) carbon footprint, on the other hand, is higher for the 'Thermomechanical-Hydro' flowsheet, mainly caused by the more extensive hydrometallurgical processing required to produce battery-grade end products and the external processing of the graphite containing leach residue, in a waste incinerator, also resulting in CO_2 emissions.

The analysis of the main drivers in this study enables us to identify the critical choices that need to be carefully defined when looking at the impact of end-of-life lithium-ion module recycling: First, a clear description of each output stream and its fate, taking into account waste legislations; second, the choice of the avoided products datasets, ensuring the geographical representativeness matches the scope of the study; third, a clear reporting of the burden and credits to facilitate comparison of different studies.

This study also clearly highlights that both 'Pyro-Hydro' and 'Thermomechanical-Hydro' flowsheets have their challenges but also opportunities for decarbonization and show that improvements in graphite and electrolyte recycling are essential to make battery recycling more sustainable.

Author Contributions: Investigation, G.V.H. and B.R.; Methodology, G.V.H.; Validation, B.V.; Writing—original draft, G.V.H., B.R. and B.V.; Writing—review and editing, G.V.H. All authors have read and agreed to the published version of the manuscript.

Funding: This research received no external funding.

Data Availability Statement: Data are contained within the article.

Conflicts of Interest: The authors declare no conflict of interest. All authors are employed by Umicore. The remaining authors declare that the research was conducted in the absence of any commercial or financial re-lationships that could be construed as a potential conflict of interest.

References

1. Gregoir, L.; Van Acker, K. Metals for Clean Energy. 2023. Available online: https://eurometaux.eu/metals-clean-energy/ (accessed on 4 May 2023).
2. Pinegar, H.; Smith, Y.R. Recycling of End-of-Life Lithium Ion Batteries, Part I: Commercial Processes. *J. Sustain. Metall.* **2019**, *5*, 402–416. [CrossRef]
3. Regulation (EU) 2023/1542 of 12 July 2023 Concerning Batteries and Waste Batteries, Amending Directive 2008/98/EC and Regulation (EU) 2019/1020 and Repealing Directive 2006/66/EC. Available online: https://eur-lex.europa.eu/legal-content/EN/TXT/PDF/?uri=CELEX:32023R1542 (accessed on 4 May 2023).
4. Global Battery Alliance. GBA Battery Passport Greenhouse Gas Rulebook. 2023. Available online: https://www.globalbattery.org/publications/ (accessed on 4 May 2023).
5. Cheret, D.; Santen, S. Battery Recycling. European Patent EP1589121 B1, 31 December 2008.
6. Velázquez-Martinez, O.; Valio, J.; Santasalo-Aarnio, A.; Reuter, M.; Serna-Guerrero, R. A Critical Review of Lithium-Ion Battery Recycling Processes from a Circular Economy Perspective. *Batteries* **2019**, *5*, 68. [CrossRef]
7. Brückner, L.; Frank, J.; Elwert, T. Industrial Recycling of Lithium-Ion Batteries—A Critical Review of Metallurgical Process Routes. *Metals* **2020**, *10*, 1107. [CrossRef]
8. Doose, S.; Mayer, J.K.; Michalowski, P.; Kwade, A. Challenges in Ecofriendly Battery Recycling and Closed Material Cycles: A Perspective on Future Lithium Battery Generations. *Metals* **2021**, *11*, 291. [CrossRef]

9. Scheunis, L.; Callebaut, W. Process for the Recovery of Lithium. European Patent EP3884076 B1, 7 September 2022.
10. Umicore Capital Markets Day. 2022. Available online: https://www.umicore.com/en/investors/capital-markets-day/ (accessed on 4 May 2023).
11. Rajaeifar, M.A.; Raugei, M.; Steubing, B.; Hartwell, A.; Anderson, P.A.; Heidrich, O. Life cycle assessment of lithium-ion battery recycling using pyrometallurgical technologies. *J. Ind. Ecol.* **2021**, *25*, 1560–1571. [CrossRef]
12. Kallitsis, E.; Korre, A.; Kelsall, G.H. Life cycle assessment of recycling options for automotive Li-ion battery packs. *J. Clean. Prod.* **2022**, *371*, 133636. [CrossRef]
13. Neuman, J.; Petranikova, M.; Meeus, M.; Gamarra, J.D.; Younesi, R.; Winter, M.; Nowak, S. Recycling of Lithium-Ion Batteries–Current State of the Art, Circular Economy, and Next Generation Recycling. *Adv. Energy Mater.* **2022**, *12*, 2102917. [CrossRef]
14. Directive 2008/98/EC of the European Parliament and of the Council of 19 November 2008 on Waste and Repealing Certain Directives. Available online: https://eur-lex.europa.eu/legal-content/EN/TXT/?uri=celex%3A32008L0098 (accessed on 14 March 2023).
15. Cobalt Institute. *Life Cycle Inventory and Life Cycle Assessment of Refined Cobalt: Final Report*; Cobalt Institute: Guildford, UK, 2015.
16. Nickel Institute. Life Cycle Assessment of Nickel Product, Reference Year 2017: Final Report; May 2020. Available online: https://nickelinstitute.org/en/policy/nickel-life-cycle-management/nickel-life-cycle-data/ (accessed on 14 March 2023).
17. *Ecoinvent Data*; v3.4; Swiss Centre for Life Cycle Inventories: Dübendorf, Switzerland, 2017.
18. Commission Recommendation 2021/2279 of 15 December 2021 on the Use of the Environmental Footprint Methods to Measure and Communicate the Life Cycle Environmental Performance of Products and Organisations. Available online: https://eur-lex.europa.eu/legal-content/EN/TXT/?uri=CELEX%3A32021H2279 (accessed on 14 March 2023).
19. Commission Recommendation 2013/179/EU of 9 April 2013 on the Use of Common Methods to Measure and Communicate the Life Cycle Environmental Performance of Products and Organisations. Available online: https://eur-lex.europa.eu/legal-content/EN/TXT/PDF/?uri=CELEX:32013H0179 (accessed on 14 March 2023).
20. World Business Council for Sustainable Development and World Resources Institute. The Greenhouse Gas Protocol: A Corporate Accounting and Reporting Standard. 2004. Available online: https://ghgprotocol.org/sites/default/files/standards/ghg-protocol-revised.pdf (accessed on 10 November 2023).
21. *ISO 14044:2006*; ISO 14044:2006/Amd 2:2020, Environmental Management—Life Cycle Assessment—Requirements and guidelines Amendment 2. ISO: Geneva, Switzerland, 2020.
22. Dai, Q.; Kelly, J.C.; Dunn, J.; Benavides, P.T. Update of Bill-of-Materials and Cathode Materials Production for Lithium-Ion Batteries in the GREET® Model, Argonne National Laboratory. 2018. Available online: https://greet.es.anl.gov/files/update_bom_cm (accessed on 4 May 2023).
23. Liu, J.; Shi, H.; Hu, X.; Geng, Y.; Yang, L.; Shao, P.; Luo, X. Critical strategies for recycling process of graphite from spent lithium-ion batteries: A review. *Sci. Total Environ.* **2022**, *816*, 151621. [CrossRef]
24. Rey, I.; Vallejo, C.; Santiago, G.; Iturrondobeitia, M.; Lizundia, E. Environmental Impacts of Graphite Recycling from Spent Lithium-Ion Batteries Based on Life Cycle Assessment. *ACS Sustain. Chem. Eng.* **2021**, *9*, 14488–14501. [CrossRef]
25. Mohr, M.; Peters, J.F.; Baumann, M.; Weil, M. Toward a cell-chemistry specific life cycle assessment of lithium-ion battery recycling processes. *J. Ind. Ecol.* **2020**, *24*, 1310–1322. [CrossRef]
26. Buchert, M.; Sutter, J. Aktualisierte Ökobilanzen zum Recyclingverfahren LithoRec II für Lithium-Ionen-Batterien (Stand 09/2016). 2016. Available online: https://www.erneuerbar-mobil.de/sites/default/files/2017-01/LithoRec%20II-LCA-Update%202016.pdf (accessed on 14 March 2023).
27. *Ecoinvent Data*; v3.1; Swiss Centre for Life Cycle Inventories: Dübendorf, Switerzerland, 2014.